Supporting information

Enhancing the Crystallization and Optimizing Orientation of Perovskites Film via Controlling Nucleation Dynamics

Qiuju Liang, Jiangang Liu, Zhongkai Cheng, Yan Li, Liang Chen, Rui Zhang, Jidong Zhang and Yanchun Han*

State Key Laboratory of Polymer Physics and Chemistry, Changchun Institute of Applied Chemistry, Chinese Academy of Sciences, 5625 Renmin Street, Changchun 130022, P. R. China; Email: ychan@ciac.ac.cn; Fax: 86-431-85262120 ; Tel: 86-431-85262120

University of the Chinese Academy of Sciences, No.19A Yuquan Road, Beijing 100049, P. R. China.
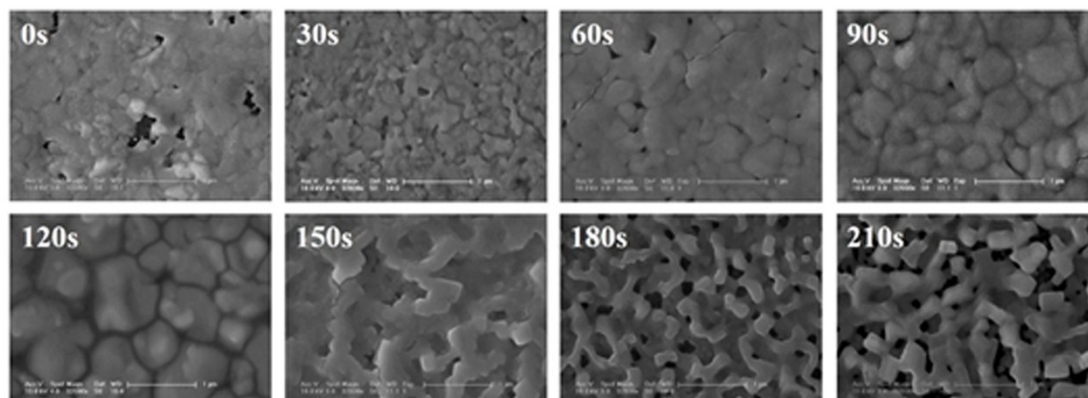
Fig. S1

Fig. S1 Low-magnification and high-magnification SEM top-view images of perovskite films treated by IPA with different time. All the films are thermal annealed 5 h at 75 °C.
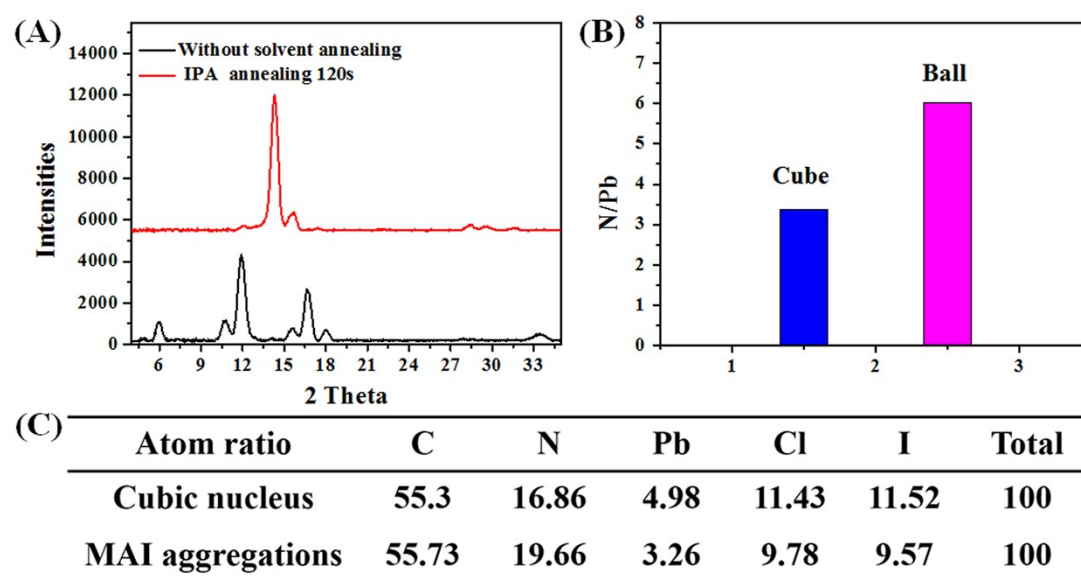
Fig. S2

Atom ratio	C	N	Pb	Cl	I	Total
Cubic nucleus	55.3	16.86	4.98	11.43	11.52	100
MAI aggregations	55.73	19.66	3.26	9.78	9.57	100

Fig. S2 (A) The out of plane XRD of the spin-coated film and film with IPA vapor annealed 120s placed under vacuum 2h. Both of the film are without thermal annealing. (B) The bar graph of atom ratio of nitrogen to lead elements in the cubic crystals (blue one) and big round aggregations (purple one) based on the elements analysis table shown in Table S 2(C). (C) The atom ratio of the cubic nucleus and MAI aggregations seen in Fig. 4.

As Fig. S2 (A) show, only peaks assigned to lead halide and the coordinated compound of Pb^{2+} with N, N-dimethylformamide (DMF) can be observed in the pristine film shown in Fig. S2 (A). While, after SSA treatment, intense signals for perovskite are visible, indicating the formation of perovskite. In addition, the energy dispersive spectroscopy (EDS) results (Fig. S2 (B)) shows there are more nitrogen element in the balls than the cubes, which implies the balls came from the aggregation of MAI (the elements distribution is shown in S2 (C)).
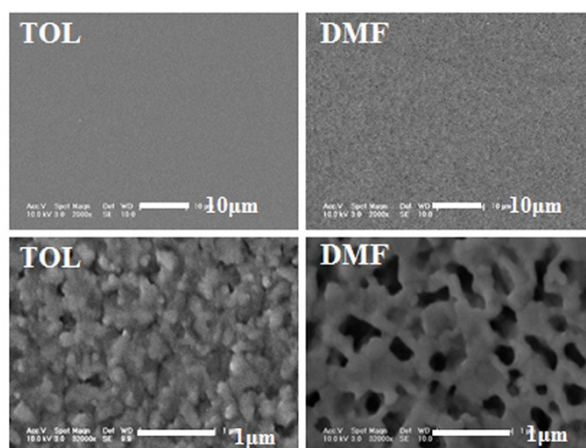
Fig. S3

Fig. S3 SEM images of top surface of $CH_3NH_3PbI_3Cl_{3-x}$ films treated with TOL 180s and DMF 20s.

The different TOL vapor annealing times rarely affect the film morphology. Moreover, short DMF vapor annealing time produces nonuniform film, but long DMF annealing time produces film with lots of uncovered holes. Therefore, the selective solubility of IPA (the solubility of lead halide and MAI in different solvent are shown in Table S4) is the key function to optimize the film morphology.

Table S4

S(g/ml)	DMF	IPA	TOL
MAI	1061.25	77.92	<0.005
PbCl$_2$	17.34	<0.006	<0.002
PbI$_2$	787.43	<0.008	<0.004

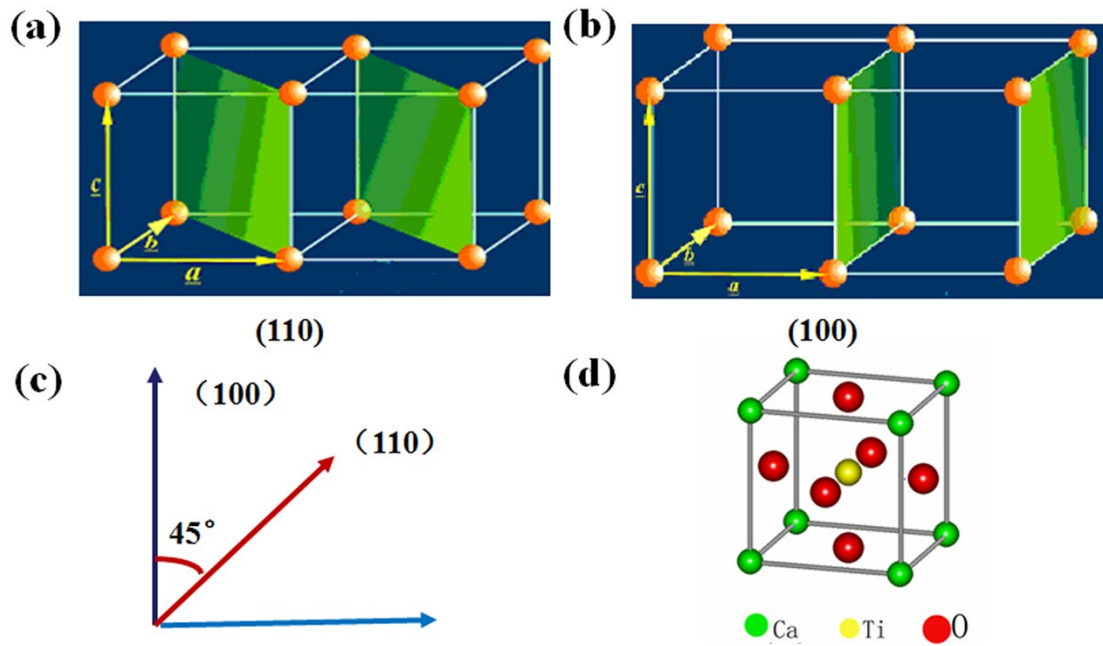**Table S4** The solubilities of MAI, PbI$_2$ and PbCl$_2$ in different solvents.

Fig. S5

Fig. S5 (a) (b) the schematic diagram of (100) and (110) lattice plane. (c) The dihedral angle relationship of the (100) and (110) lattice plane. (d) The crystal cell of perovskites.

According to the dihedral angel relationship of the $(h\ k\ 0)$ $(h = k)$ and $(h\ 0\ 0)$ lattice planes in orthorhombic crystal system, it is obvious that when the azimuthal angle of (110) lattice plane is 45°, the (100) lattice plane would perpendicular to the substrate.
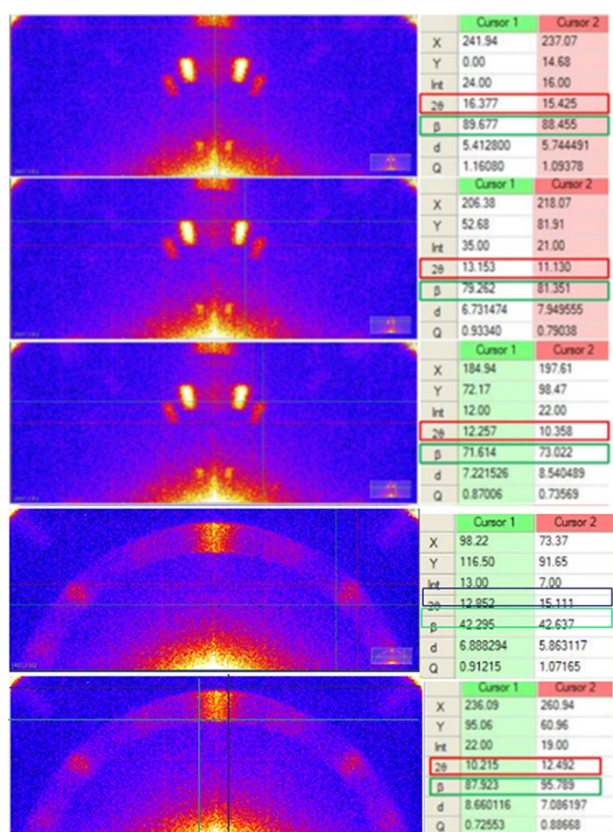
Fig. S6

Fig. S6 The location of the two-dimensional GIXD signals of Fig. 5.
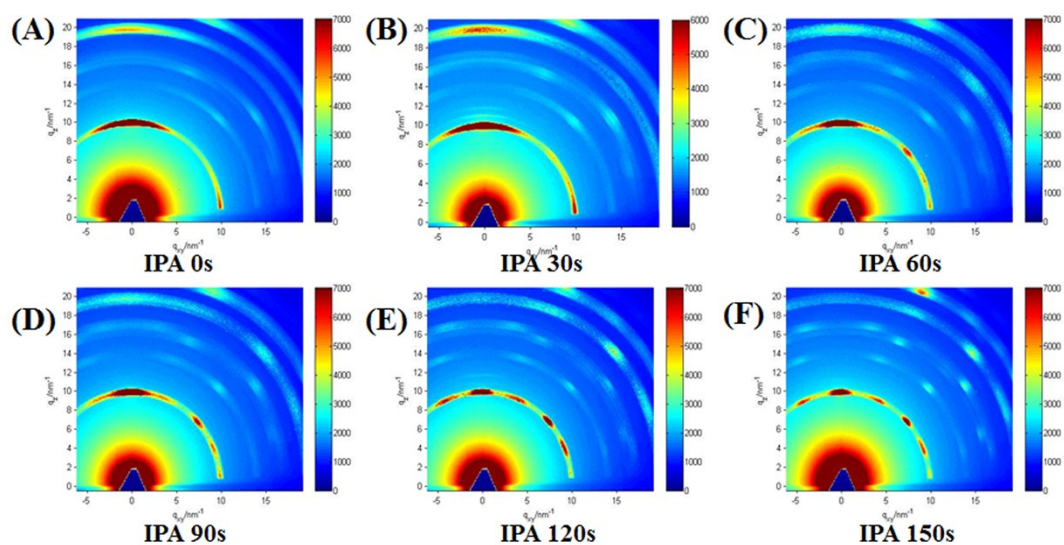
Fig. S7

Fig. S7 The two-dimensional GIXD images of $CH_3NH_3PbI_{3-x}Cl_x$ films without and with IPA vapor annealing different times.

Combining the Fig. S7 and Fig. 2, we can conclude that it is essential for optimizing the film morphology and crystal orientation to form uniformly distributed nucleus.
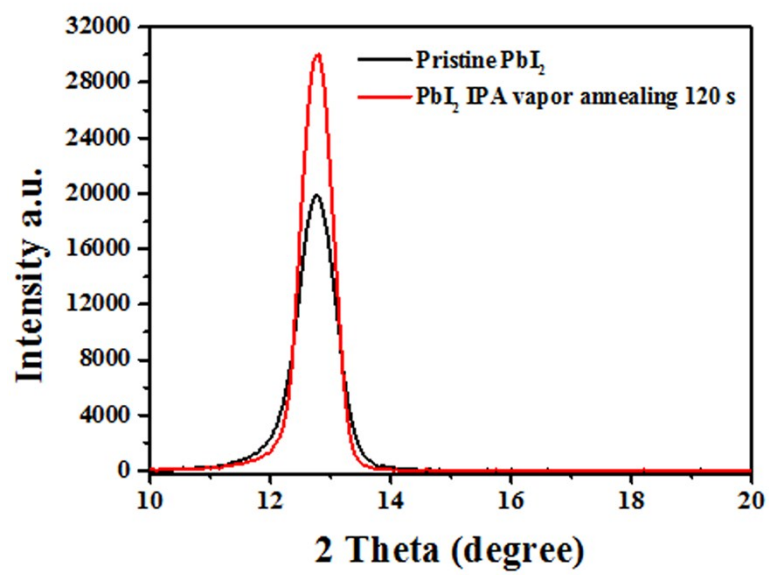
Fig. S8

Fig. S8 The out of plane XRD profile shows the crystallinity of pristine pure PbI_2 film and pure PbI_2 film with IPA vapor annealing (120 s).

Table S9

	Voc (V)	Jsc (mA/cm2)	FF	PCE (%)
Without annealing	0.92	14.68	0.67	9.05
IPA annealing 90s	0.93	16.41	0.71	11.21
IPA annealing 120s	0.95	17.43	0.74	12.25
IPA annealing 150s	0.96	13.32	0.58	7.42

Table S9 Parameters of the device performance without and with IPA vapor annealing treatments under 100 mW cm^{-2} simulated AM1.5G illumination.
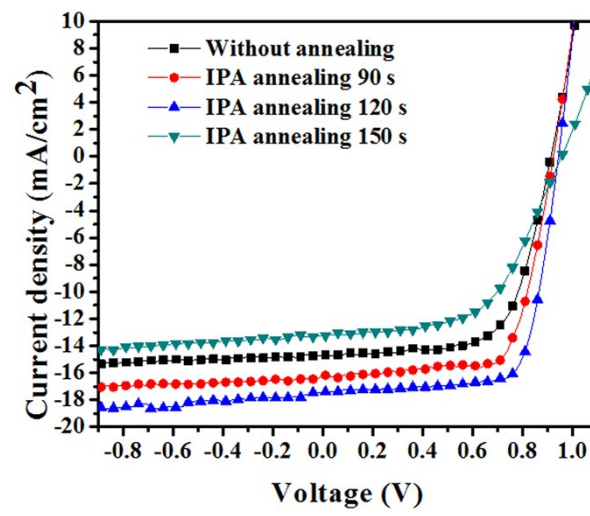
Fig. S10

Fig. S10 *J-V* curves for the devices without and with IPA vapor annealing different time.
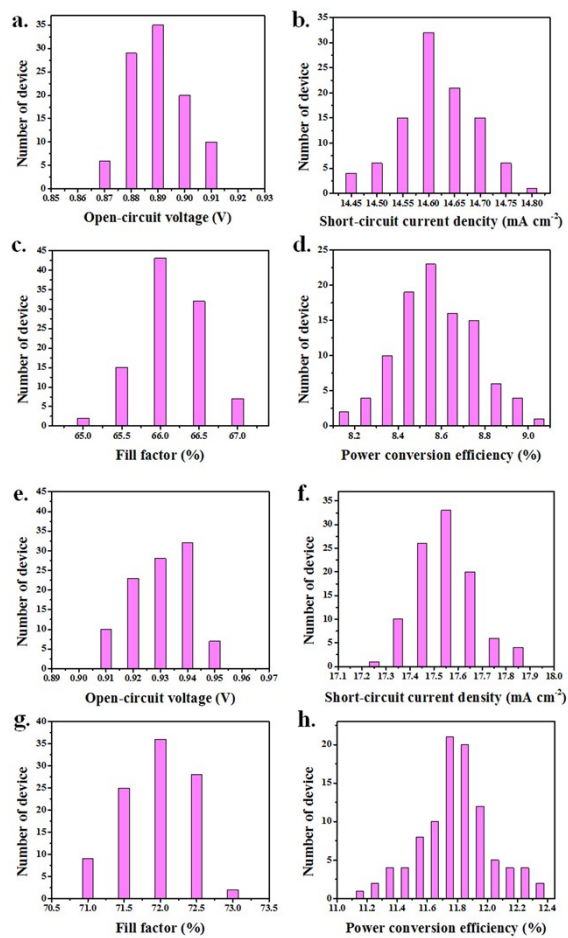
Fig. S11

Fig. S11 The parameter histogram of device based on pristine film and treated film: a, b, c and d the *V*oc, *J*sc, *FF* and PCE histograms of device based on pristine film; e, f, g and h the *V*oc, *J*sc, *FF* and PCE histograms of device based on treated film.
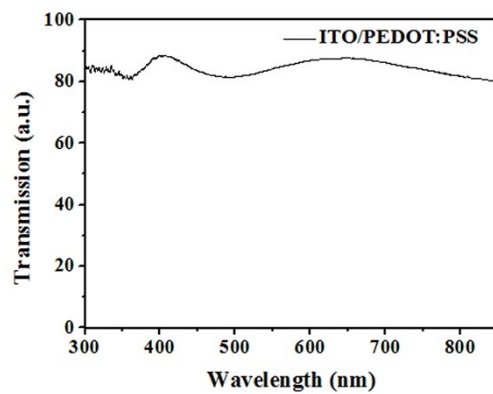
Fig. S12

Fig. S12 The absorption spectra of ITO/PEDOT:PSS.